Journal of Electroanalytical Chemistry 703 (2013) 158–165

Contents lists available at SciVerse ScienceDirect

Journal of Electroanalytical Chemistry

journal homepage: www.elsevier.com/locate/jelechem

Study of the effects of surface pK_a and electron transfer kinetics of electroactive 4-nitrothiophenol/4-mercaptobenzoic acid binary SAM on the simultaneous determination of epinephrine and uric acid

Danielle Diniz Justino [a], Ana Luísa Almeida Lage [a], Dênio Emanuel Pires Souto [a], Jussara Vieira da Silva [a], Wallans Torres Pio dos Santos [b], Rita de Cássia Silva Luz [a], Flavio Santos Damos [a,*]

[a] Instituto de Ciência e Tecnologia, Universidade Federal dos Vales do Jequitinhonha e Mucuri, 39100-000 Diamantina – MG, Brazil
[b] Departamento de Farmácia, Universidade Federal dos Vales do Jequitinhonha e Mucuri, 39100-000 Diamantina – MG, Brazil

ARTICLE INFO

Article history:
Received 20 February 2013
Received in revised form 22 April 2013
Accepted 26 May 2013
Available online 6 June 2013

Keywords:
Surface pK_{ap}
Epinephrine
Uric acid
Mixed self-assembled monolayer
Scanning electrochemical microscopy

ABSTRACT

In the present paper, the use of a gold electrode modified by 4-nitrothiophenol/4-mercaptobenzoic acid binary self-assembled monolayer (4NTP/4MBA SAM) for the simultaneous determination of epinephrine (EP) and uric acid (UA) is described. Electron transfer (ET) kinetics through 4NTP/4MBA SAM was studied using scanning electrochemical microscopy (SECM) and electrochemical impedance spectroscopy (EIS). The SECM strategy was used to measure the heterogeneous rate constant for activated 4NTP/4MBA SAM and non-activated 4NTP/4MBA SAM using $[Fe(CN)_6]^{4-/3-}$ as probe. The apparent surface pK_{ap} value of the 4NTP/4MBA SAM modified electrode was estimated by EIS (pK_{ap} = 5.0). The electrochemical response of the modified electrode toward epinephrine (EP) and uric acid (UA) were investigated by differential pulse voltammetry (DPV). The results showed an efficient electrochemical response and surface activity of the electrode for the electro-oxidation of EP and UA, which leads to improvement of selectivity of the electrode response. Two well-defined voltammetric peaks, in a buffered solution at pH 5.5, were obtained by differential pulse voltammetry (DPV) at 0.120 and 0.475 V vs Ag/AgCl for EP and UA, respectively. Linear calibration plots were obtained in the range of 0.1–2.0 μmol L^{-1} for EP and 1–175 μmol L^{-1} for UA, with sensitivity of 1.2 μA L μmol^{-1} and 0.0117 μA L μmol^{-1}, respectively.

1. Introduction

The development and application of electrochemical sensors have been a research of considerable interest in nowadays [1–3]. The concept of modified electrodes is one of the most exciting developments in the field of sensors. Thus, a number of different strategies have been employed for the modification of the electrode surface. Among them, self-assembled monolayers (SAMs) are of prime interest in electrochemistry, as the presence of molecules chemically bound to the surface renders the properties of the modified interface (i.e., wetting, conductivity, adhesion, and chemistry properties) to be entirely different than those of the bare substrate [4,5]. The exposed terminal functional group(s) of the SAM can be further modified so as to enhance or to alter the monolayer properties.

Therefore, the SAMs have recently become very important due to their potential applications to molecular and biomolecular recognition [6], lithography resists [7], sensing and electrode modification [8], corrosion prevention [9], and other areas where tailoring the physicochemical properties of an interface is required. With functional groups at their outer surface to which electron donors or acceptors could be attached, such monolayers would offer an ideal starting place in the construction of electron-transfer models [4]. The possibility to generate surfaces containing electroactive relevant functionalities is certainly one of the most exciting properties of SAMs, due to their ability of binding of specific functional head groups with variety of chemical and biological species in solution. In particular, redox-active SAMs provide an excellent platform for exploiting electrochemistry to improve electron transfer processes [10,11].

On the other hand, there has been enormous interest in designing highly selective interfaces for use in sensing and separation technology [12]. In this sense, the interfacial proton transfer studies are crucial to understand and control acid/base properties of surface confined molecules and are essential to applications including fundamental studies of interfacial phenomena [13]. Most of the molecular recognition systems often presented rely on the binding interaction of target analytes with the ionizable terminal groups of thiols [14].

* Corresponding author. Tel.: +55 38 3532 1283; fax: +55 38 3532 1223.
E-mail address: flavio.damos@ufvjm.edu.br (F.S. Damos).

1572-6657/$ - see front matter © 2013 Elsevier B.V. All rights reserved.
http://dx.doi.org/10.1016/j.jelechem.2013.05.024

In this sense, the development of two-component self-assembled monolayers on gold provides a convenient, flexible, and simple method to control the interfacial properties of metal electrodes combining electroactivity and selectivity in the same monolayer. Thus, the use of mixed self-assembled monolayer modified electrodes can improve the selectivity and sensitivity of gold electrodes. Apart from selectivity, binary electroactive/selective self assembled monolayer can enhances the response time and the stability as compared to other surface modification techniques in the development of electrochemical sensors.

Neurotransmitters are the primary chemical messengers released from neurons and relay, amplify and modulate signals to other cells [13–16]. Due to the significant contribution of neurotransmitters to not only neurological functioning, but also endocrinological and immunological actions, clinicians and researchers are interested in the function and measurement of neurotransmitters as they have the potential to serve as clinically relevant biomarkers for specific disease states or to monitor treatment efficacy [17]. Neurotransmitters are present throughout the body and represented by research demonstrating measurements in various biological fluids, including serum, plasma, platelets, cerebral spinal fluid (CSF), saliva, and urine [18].

Epinephrine (EP) is an important neurotransmitter in mammalian central nervous systems, and it exits in the nervous tissue and body fluid in the form of organic cations [19]. Epinephrine is employed in cardiac resuscitation and, due to its vasoconstrictive properties, it is also added to local anesthetics to retard systemic absorption and prolong effect. It works by narrowing the blood vessels, increasing blood pressure and blood glucose levels and the changes of its concentration may result in many diseases [18,19]. Till date, the ability to detect EP with high selectivity and sensitivity is of high interest in electroanalytical research. Therefore, the determination of EP has been reported using chromatographic methods [20], spectroscopic methods [21], chemiluminescence [22], capillary electrophoresis [23], flow injection analysis [24], and electrochemical methods [25–27].

UA or urate is the primary end product of purine metabolism. Elevated UA levels in biological fluids are related to several diseases such as pneumonia, leukemia, hyperuricemia, gout and Lesch-Nyhan syndrome [28]. Its normal level in blood is about 34–85 μmol L^{-1} and in urine about 570–3400 μmol L^{-1} [29]. Hence, it is desirable to develop a simple and direct method for monitoring the concentration of UA.

EP and UA are coexistent in biological fluids of human, so the simultaneous detection of EP and UA in a mixture is quite attractive to a number of researches. The major challenge in EP and UA simultaneous analysis is the elimination of interferences from ascorbic acid (AA). The UA and AA oxidation peaks are very close to that of EP which often results in peak overlapping [30,31]. Therefore, a lot of chemically-modified electrodes have been developed to eliminate the interference of UA and AA to EP determination [32]. However, each method has often suffered from disadvantage with regard to sensitivity toward EP determination in presence of UA and AA.

In this context, the present work reports the development of an efficient, sensitive, selective and stable sensor combined with the capability to detect low EP concentrations. The present work describes aspects of the application of a binary self-assembled monolayer based on 4-nitrothiophenol (4NTP)/4-mercaptobenzoic acid (4MBA) toward selective and sensitive interaction with epinephrine and uric acid in presence of ascorbate. In this sense, the effects of surface pK_a and electron transfer kinetics of the mixed SAM were exploited to improve the sensitivity and selectivity of the binary SAM.

2. Experimental

2.1. Chemicals

All chemicals were of analytical grade and were used as received without further purification. 4-mercaptobenzoic acid (4MBA), 4-nitrothiophenol (4NTP), potassium hexacyanoferrate, uric acid and epinephrine were acquired from Sigma–Aldrich (St. Louis, MO, USA). Ascorbic acid, ethanol (99.5%), sulfuric acid and monobasic sodium phosphate were acquired from Vetec Química Fina (Rio de Janeiro, RJ, Brazil). Deionized water was used after purification in a Milli Q system and the actual pH of the solutions was determined with a Corning pH/ion analyzer model 350.

2.2. Preparation of substrate and self assembled monolayer modified electrode

A gold electrode was polished with alumina slurries (particle diameters, 1.0 and 0.05 μm) and rinsed with pure water. The electrode was washed by dipping in an aqueous 0.05 mol L^{-1} H_2SO_4 and subsequently scanned from −0.4 to +1.5 V for 10 times (scan rate, 100 mV s^{-1}). Finally, the electrode was immersed in a piranha solution (a mixture with 3:1 of concentrated sulfuric acid and 30% hydrogen peroxide) for 1 min.

For the immobilization of 4MBA or 4NTP single self-assembled monolayer, the gold electrode was immersed in a 1.0 mmol L^{-1} solution of 4MBA or 4NTP in ethanol for 24 h. The electrode was removed from the solution and rinsed with copious amounts of ethanol and water and immediately used in the electrochemical experiments. The modification of gold surface with mixed self-assembled monolayer was carried out by immersion of the electrode in an ethanolic solution containing a mixture of 1.0 mmol L^{-1} 4NTP and 1.0 mmol L^{-1} 4MBA for 24 h. Finally, the modified electrode was thoroughly rinsed with distilled ethanol and placed into the electrochemical cell.

2.3. Electrochemical and scanning electrochemical microscopy measurements

Cyclic voltammetry and differential pulse voltammetry were performed with an AUTOLAB potentiostat model PGSTAT 128N equipped with FRA 2 module from Eco chemie (Utrecht, Netherlands) coupled to a PC microcomputer with GPES 4.9 software. An electrochemical cell containing 10.0 mL of buffer solution with an Ag/AgCl (sat.), KCl 3 mol L^{-1} as reference, a Pt wire as auxiliary and a modified gold (3 mm diameter) as working electrode were used for all measurements. The impedance data were analyzed by non-linear least squares (NLLSs) using the EQUIVCTR.PAS program by Boukamp [33]. Theory validation of the EIS data was performed applying the Kramers–Kronig test using software from the AUTOLAB electrochemical system. A sinusoidal potential modulation of 10 mV amplitude was superimposed on a fixed d.c. potential and the amplitude and phase angle of the resulting current were recorded at frequencies ranging from 100 kHz to 0.1 Hz.

All SECM approach curves were carried out using the feedback mode of SECM with a CHI 920C microscope (CH Instruments) in a four-electrode configuration at room temperature which uses a combination of stepper motors positioners of resolution of 8 nm with 50 mm travel distance and an XYZ piezo block in order to position the tip. The electrochemical cell employed was built in Teflon with an 8 mm diameter aperture. SECM tips were ultramicroelectrodes (UMEs) of Pt with radius, a, of 10 μm and RG ~5 (RG is the ratio of the insulating glass radius, rg, to that of a, so RG = rg/a), which were constructed and characterized as previously

described. Approach curves were recorded by moving the tip toward the modified electrode surface at the speed of 2 μm s^{-1} while the tip was held at a constant potential for a diffusion-limited current of solution-phase electrochemical probe at the tip.

3. Results and discussion

3.1. Electrochemical behavior of the 4NTP/4MBA SAM

Cyclic voltammograms of gold electrodes modified with 4NTP/4MBA SAM were carried out in 0.1 M phosphate buffer (pH 7.0) at 50 mV s^{-1} over the potential range of +0.50 to −0.60 V (Fig. 1). On the first cathodic scan (solid line) one well-resolved, chemically irreversible process is observed at peak potential value of −0.52 V. Upon scan reversal at −0.60 V, an anodic wave with a peak potential centered at −0.05 V is observed. On the second (dashed line) and subsequent potential scans, an additional cathodic peak was observed at −0.08 V which is the cathodic counterpart to the anodic wave at −0.05 V. This appears to indicate that the first cathodic sweep gives rise to a reversible redox couple with a formal potential of −0.065 V. In addition, the peak current of the cathodic wave centered at −0.52 decreased significantly on the second and on subsequent scans.

Fig. 1 shows cyclic voltammograms of the SAM activation process obtained under optimized conditions. As can be seen in Fig. 1, in the first cycle the nitro-group is irreversibly reduced to R-NHOH and oxidized to R-NO in the back scan. In the second cycle is possible to observe a defined redox peak that can be attributed to R-NO/R-NHOH redox couple.

On the basis of these results, we propose that for electrodes modified with 4NTP, when the potential is held at −0.52 V in pH 7.0 phosphate buffer, an irreversible four-electron, four-proton electrochemical reduction of each of the nitro groups of 4NTP takes place according to the mechanism presented in Eq. (1) previously proposed for others nitro-thiols by Kemula and co-workers [34], by Lindbeck and Freund [35], and Casero and co-workers [36] who carried out studies at gold-electrode surfaces.

$$\text{Au-SC}_6\text{H}_6\text{-NO}_2 + 4\text{H}^+ + 4\text{e}^- \rightarrow \text{Au-SC}_6\text{H}_6\text{-NHOH} + \text{H}_2\text{O} \quad (1)$$

In the second cycle is possible to observe a defined redox process that can be attributed to –NO/–NHOH redox couple.

$$\text{Au-SC}_6\text{H}_6\text{-NO} + 2\text{H}^+ + 2\text{e}^- \leftrightarrow \text{Au-SC}_6\text{H}_6\text{-NHOH} \quad (2)$$

After SAM activation process, the potential range around the –NO/–NHOH redox couple was selected and cyclic voltammograms were recorded at various scan rates (10–1000 mV s^{-1}). Inset of Fig. 1 shows the cyclic voltammograms of 4NTP/4MBA SAM modified electrode obtained in phosphate buffer solution (pH 7.0) at various potential scan rates. As can be seen, the cyclic voltammograms exhibits one pair of reduction and oxidation peak currents in each cycle. This suggested two-electron transfer process in one step, as previously reported in literature [34–36]. In the anodic scan, the cyclic voltammogram exhibits an anodic peak at forward scan of potential related to the oxidation of Au-SC_6H_6-NHOH, whereas the reverse scan presents a cathodic peak related to reduction of Au-SC_6H_6-NO.

The peak currents of both redox couples were directly proportional to the scan rates, which is characteristic of the adsorptive process at the electrode surface or a surface confined redox process [37]. Further, the ratio of anodic peak current to the cathodic peak current (I_{pa}/I_{pc}) was almost equal the unity, the peak potential did not alter with the increase of scan rate (data not shown).

As can be seen in Inset of Fig. 1a, the cyclic voltammogram of activated SAM exhibits an anodic peak at −0.05 V in the forward potential scan, and a cathodic peak at −0.083 V in the reverse scan.

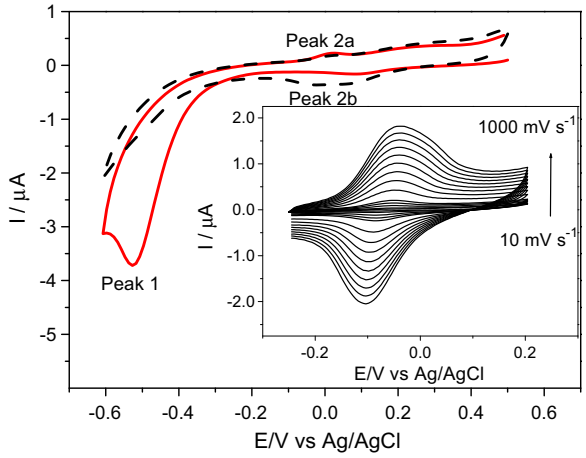

Fig. 1. (a) Cyclic voltammograms at 50 mV s^{-1} of an Au electrode modified with a binary 4NTP/4MBA monolayer in 0.1 mol L^{-1} phosphate buffer (pH 7.0) in the potential range from +0.5 to −0.6 V (activation process of binary SAM). Inset: cyclic voltammograms of 4NTP/4MBA SAM modified electrode in 0.1 mol L^{-1} phosphate buffer solution (pH 7.0) at potential scan rates of 0.01–1 V s^{-1} (after activation process).

For an ideal nernstian adsorptive electrochemical reaction under Langmuir isotherm conditions, $Ep_a = Ep_c$ ($\Delta Ep = 0$). Half wave potential ($E_{1/2}$), ΔEp (the difference between Ep_a and Ep_c) and the total width at half-height ($\Delta Ep_{,1/2}$) were −0.065 V vs Ag/AgCl, −0.033 V and 0.09 V, respectively. This $\Delta Ep_{,1/2}$ value is larger than the theoretically expected value of 91 mV/n (=45 mV, with $n = 2$) mV at 25 °C, which may be caused by the existence of redox centers in different environments. Therefore, the redox couple Au-SC_6H_6-NHOH/Au-SC_6H_6-NO in 4NTP/4MBA SAM shows a quasi-reversible behavior in phosphate buffer solution pH 7.0 [37].

An approximate amount of the electroactive species was estimated by the method suggested by Bard and Falkner [37]. According to this method the peak current is related to the surface concentration on the electroactive species, Γ, as in following equation:

$$I_p = \frac{n^2F^2A\Gamma v}{4RT} \quad (3)$$

where n represent the number of electrons involved in the reaction, A is the surface area of the electrode (cm^2), Γ (mol cm_2) is the surface coverage and other symbols have their usual meanings. From the slope (1.40×10^{-6} A s V^{-1} from Inset of Fig. 1) of anodic peak currents vs scan rate, the calculated surface concentration of 4NTP was approximately 5.25×10^{-12} mol cm^{-2}.

A number of electrochemical methods and techniques have been used to allow the quantitative determination of rate constants for electron transfer processes, including Laviron method, Marcus density of states theory, alternating current voltammetry (ACV), electrochemical impedance spectroscopy and scanning electrochemical microscopy. The advantages and limitations of each of these techniques in electrochemistry of redox self-assembled monolayers have been evaluated by Meade et al. [4].

Transient electrochemical techniques, like cyclic voltammetry and chronoamperometry, have been most commonly used for measuring the rates of ET through alkanethiol monolayers. However, these methods are burdened by the effects the resistive potential drop and double layer charging current, which affect the reliability of the results and decrease the upper limit for the measurable rate constant [38,39]. In Laviron's method, the values of k^o_{ET} have been determined by measuring the peak separation between the reduction and oxidation peaks [40]. However, for relatively fast ET, the peak separation will be too small to give a reliable indicator

of k^o_{ET}, requiring that faster scan rates be used to increase the peak potential separation. As can be seen in Inset of Fig. 1, at a scan rate of 1000 mV s^{-1} was verified ΔEp ($Epa - Epc$) of 60 mV which is much lower than 200 mV such as the Laviron's methods cannot applied.

In this sense, the scanning electrochemical microscopy (SECM) was used to extract a value of k^o_{ET} for adsorbed 4NTP/4MBA SAM. This technique has several advantages over CV for measuring the ET kinetics, including: (i) it simultaneously measures the bimolecular ET rate constant, k_{BI}, between redox probe and SAM and the tunneling ET rate constant, k^o_{ET}, between the SAM and the electrode, allowing more information to be extracted from a single measurement; (ii) the currents drawn by the UME are very small and the measurements are recorded at steady state, fewer problems are encountered with the *iR* drop in the lower ionic strength solution. Therefore, the transfer coefficient, α, and the apparent heterogeneous rate constant of charge transfer, k^o_{ET} between the electrode and a surface-confined redox couple were evaluated by SECM.

3.2. Effects of SAM activation on the electron transfer kinetics by scanning electrochemical microscopy

In order to investigate the effects of SAM activation on the electron transfer kinetics, SECM experiments were carried out by using a Pt disk ultramicroelectrode as a probe for $[Fe(CN)]^{4-}$ (Fig. 2).

Fig. 3 shows the SECM approach curves obtained with 4NTP/4MBA SAM before (a) and after (b) electrochemically triggered surface confined reaction. The potential of 500 mV vs Ag/AgCl was applied on the tip to oxidize ferrocyanide ions at the diffusion limited rate. After the electrochemically triggered surface confined reaction, the regeneration of ferrocyanide ions takes place by diffusion of ferricyanide ions to the substrate through oxidation of –NHOH group on the mixed SAM and causes an increase in the feedback current at the tip. On the other hand, before the activation process, the regeneration of ferrocyanide ions takes place by diffusion to pinholes sites and direct electron transfer at the electrode surface.

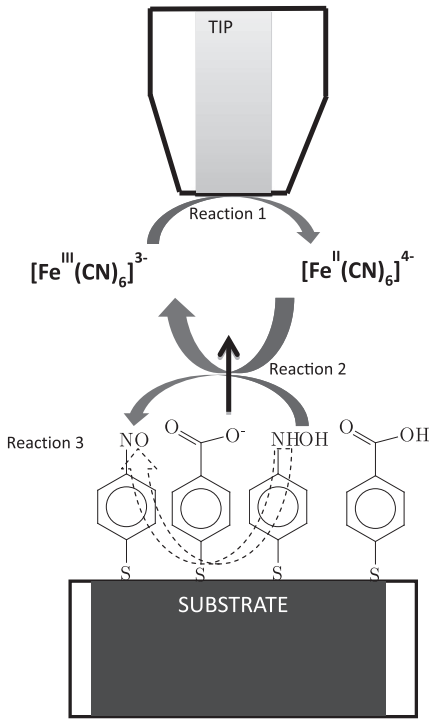

Fig. 2. Schematic view of the mediated processes involved in SECM measurements of electron transfer across activated 4MTP/4MBA SAM.

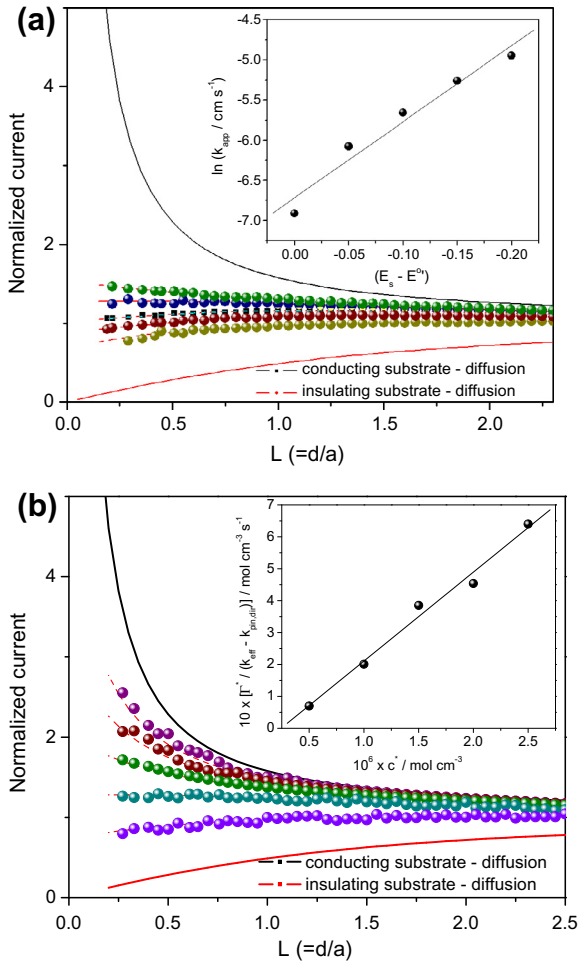

Fig. 3. SECM approach curves obtained on gold coated by a mixed monolayer of 4NTP/4MBA in a solution 0.1 mol L^{-1} phosphate buffer solution (pH 7.0). The tip was a 10 μm radius Pt disk. (a) Probe approach curves for non-activated 4NTP/4MBA at different substrate potential (from bottom to top the substrate potentials are 0, −0.05, −0.1, −0.15 and −0.2). E_{tip} = +0.5 V. Circle symbols are experimental approach curves and solid lines are theoretical curves. Insert: dependence of the k_{eff} on the substrate applied substrate potential. (b) Probe approach curves for activated 4NTP/4MBA at different concentrations of $[Fe(CN)_6^{3-}]$ (from bottom to top the ferrocyanide concentrations are 0.5, 1.0, 1.5, 2.0 and 2.5 mmol L^{-1}). Insert: dependence of the k_{eff} on the concentration of ferrocyanide.

Approach curves were collected as a function of substrate potential (E_S) for both the 4NTP/4MBA modified electrode before and after SAM activation process, while the tip potential (E_{tip}) was set to the value at which the diffusion-controlled reduction of solution phase probes of $[Fe(CN)]^{4-}$ could occur at tip (E_{tip} = 500 mV vs Ag/AgCl), and E_S was stepped to more negative values progressively (E_S = 0 mV up to −200 mV vs Ag/AgCl). According to theory, the following equations can be used to extract the first order effective heterogeneous electron transfer constant (k_{eff}) [41]:

$$I_T^k = I_S^k\left(1 - \frac{I_T^{ins}}{I_T^c}\right) + I_T^{ins} \tag{4}$$

$$I_S^k = \frac{0.78377}{L\left(1+\frac{1}{\Lambda}\right)} + \frac{\left[0.68 + 0.3315\exp\left(-\frac{1.0672}{L}\right)\right]}{\left[1 + F(L,\Lambda)\right]} \tag{5}$$

where I_T^c, I_T^k, I_T^{ins} represent the normalized tip current for diffusion-controlled regeneration of redox mediator, finite substrate kinetics,

and insulating substrate, respectively, at a normalized tip-substrate separation, $L = d/a$; I_T^k is the kinetically controlled substrate current; $\Lambda = kd/D$, where k is the apparent heterogeneous rate constant (cm/s), and $F(L,\Lambda) = (11 + 2.3\Lambda)/[\Lambda(110–40\,L)]$.

These currents are normalized by the tip current at a semi-infinite tip-substrate separation, $i_{T,\infty}$. The analytical approximations for I_T^c and I_T^{ins} [42] are:

$$I_T^c = \frac{0.78377}{L} + 0.3315\exp\left(-\frac{1.0672}{L}\right) + 0.68 \quad (6)$$

$$I_T^{ins} = \frac{1}{0.15 + \frac{1.5353}{L} + 0.58\exp\left(-\frac{1.14}{L}\right) + 0.0908\exp\left[\frac{L-6.3}{1.017L}\right]} \quad (7)$$

As Fig. 3b shows, in the case of activated 4NTP/4MBA SAM, the existence of –NO/–NHOH groups in SAM layer significantly enhanced the feedback of $[Fe(CN)_6]^{4-}$ compared to that in the absence of activation (Fig. 3a). The experimental curves were fit to theory for finite heterogeneous substrate kinetics to extract the effective rate constant (k_{eff}) for the mediated electron transfer between the 4NTP/4MBA SAM and the underlying electrode.

The activated 4NTP/4MBA SAM adsorbed on the substrate contains an electroactive group, –NHOH, and the regeneration of the mediator ($[Fe(CN)_6]^{4-}$) occurs via a bimolecular reaction with these surface-bound redox centers (Fig. 2). The reduced form of the redox mediator ($[Fe(CN)_6]^{4-}$) is oxidized at the tip electrode as shown in Fig. 2 (reaction 1). The product of this reaction ($[Fe(CN)_6]^{3-}$) diffuses to the activated 4NTP/4MBA SAM where it reacts with the reduced form of the monolayer-bound redox moieties (–NHOH) to give –NO surface group (reaction 2). Finally, the oxidized form of the monolayer-bound redox moieties (–NO) react at the substrate by the electron tunneling through the SAM to give –NHOH surface group (reaction 3). At this treatment, the overall rate constant obtained by fitting the experimental rate constant, k_{eff}, to the theory should be equal to [43]:

$$k_{eff} = \frac{k_{bi}k_f\Gamma^*}{(k_{BI}c^* + k_f + k_b)} + k_{pin,dir} \quad (8)$$

where $k_{pin,dir}$ is the rate constant for the mediator reaction at pinholes and by direct electron transfer tunneling though the 4NTP/4MBA, Γ^* is the surface concentration of redox centers in the SAM (i.e., surface concentration of –NO/NHOH), c^* is the bulk concentration of solution-phased probes, k_{BI} is the bimolecular rate constant ($mol^{-1}\,cm^3\,s^{-1}$) and k_f and k_b are the electron tunneling rate constants (s^{-1}) for forward and backward reactions respectively. At low overpotentials, when E_S is not much more negative than $E^{o\prime}_{NO/NHOH}$, $k_{BI} \gg k_f + k_b$ and Eq. (8) becomes:

$$k_{eff} = \frac{k_f\Gamma^*}{c^*} + k_{pin,dir} \quad (9)$$

In this regime, the overall rate of ET is controlled largely by the rate of tunneling between the adsorbed redox couple and the gold electrode, k_f. On the other hand, at higher overpotentials, when E_S is much more negative than $E^{o\prime}_{NO/NHOH}$, $k_{BI}\,c^* \ll k_f + k_b$ and Eq. (8) becomes:

$$k_{eff} = k_{BI}\Gamma^* + k_{pin,dir} \quad (10)$$

Under these conditions, the rate of tunneling ET is very fast as k_f increases with overpotential, according to Butler–Volmer kinetics. However, the overall rate of ET becomes limited by the bimolecular ET rate constant, k_{BI}.

To obtain an expression of k_{eff} in terms of applied substrate potential, the rate constants at one region of the substrate were fit to the Buttler–Volmer equation to obtain both the heterogeneous rate constant, k^o_{ET}, and the electron transfer coefficient, α [44]:

$$k_b = k^o_{ET}\exp[(1-\alpha)f(E_s - E_{NHOH/NO})] \quad (11a)$$

$$k_f = k^o_{ET}\exp[-\alpha f(E_s - E^o_{NHOH/NO})] \quad (11b)$$

where $f = F/RT$, F is the Faraday constant, R is the gas constant and T is the temperature.

Substituting the Butler–Volmer equations for k_f and k_b into Eq. (8), gives an overall equation to the behavior of k_{eff} as a substrate potential function, E_S [43,44]:

$$\frac{\Gamma^*}{k_{eff} - k_{pin,dir}} = \frac{c^*}{k_f} + \frac{1 + \exp\left[-\frac{F\left(E_{sub} - E^{o\prime}_{NO/NHOH}\right)}{RT}\right]}{k_{BI}} \quad (12)$$

In order to take the kinetic parameters of activated 4NTP/MBA SAM, it was used the general form of equation (Eq. (12)) for extracting k_{BI} and k_f simultaneously as suggested by Holt [45] and Salamifar et al. [46]. The Inset of Fig. 3a shows the corresponding plot of $(\Gamma^*\,k_{eff}^{-1})$ vs c^* obtained for an activated 4NTP/MBA SAM.

Experiments were carried out with $[Fe(CN)_6]^{4-}$ at concentrations of 0.5, 1.0, 1.5, 2.0 and 2.5 mmol L^{-1} in 0.1 mol L^{-1} phosphate buffer solution pH 7.0. Before each set of experiments, in order to determine Γ^* value, a voltammogram of the NTP/MBA SAM modified gold electrode at scan rate of 50 mV s^{-1} was recorded in the buffer solution. From the integration of charge of peak current, the Γ^* value for 2 electron process was obtained, and then the solution was replaced with that containing the probe. The data show a linear relationship with a slope of 2.79×10^{-4} s. The rate constants obtained were fit to Eq. (11)b and a k^o_{ET} value of $2.54 \times 10^4\,s^{-1}$ and a α value of 0.5 were obtained for activated 4NTP/4MBA SAM.

Indeed, it was necessary to assess the degree of regeneration of the ferrocyanide redox species at the substrate before activation of 4NTP/4MBA SAM to obtain the value for $k_{pin,dir}$. As discussed above, the mediator can be regenerated by reaction at defects sites in the non-activated SAM or by direct tunneling of electrons through the non-activated SAM.

The activated 4NTP/4MBA SAM modified gold electrode showed deviation from pure negative feedback at lower potentials compared to that of the non-activated 4NTP/4MBA SAM modified electrode. When the monolayer contains no redox centers capable of reacting with the mediator species, the characteristic effective rate constant reflects the contributions of the defects sites and direct tunneling of electrons through the non-activated SAM ($k_{eff} = k_{pin,dir} = k_{ET}$).

Thus, the effective rate constants obtained to non-activated 4NTP/4MBA SAM modified electrode were fitted to the Butler–Volmer equation and a k^o_{ET} value of 3.87×10^{-5} cm s^{-1} and a α value of 0.28 were obtained for non-activated 4NTP/4MBA SAM (see Inset of Fig. 3a).

Thus, considering the significant enhanced feedback of approach curves after SAM activation, it is evident that electrochemically triggered surface confined reaction is of high importance on the mixed SAM blocking properties.

3.3. Determination of apparent surface pK_a (pK_{ap}) of 4NTP/4MBA SAM

The surface pK_{ap} of the SAM of 4-mercaptobenzoic acid, SAM of 4-nitrothiophenol as well as of the binary monolayer of 4NTP/4MBA were investigated by electrochemical impedance spectroscopy. Fig. 4 shows that the impedance for the binary 4NTP/4MBA SAM is pH dependent. The titration curve of the impedance for the mixed self-assembled monolayer is plotted as a function of solution pH, as shown in inset of Fig. 4.

At very low pH (pH < 4.5) the acid group is completely protonated; therefore no electrostatic repulsive interactions between the 4NTP/MBA SAM modified Au electrode and $[Fe(CN)_6]^{3-}$ are expected. The repulsive force increased with pH, indicating that the carboxylic acid group is gradually deprotonated as the pH

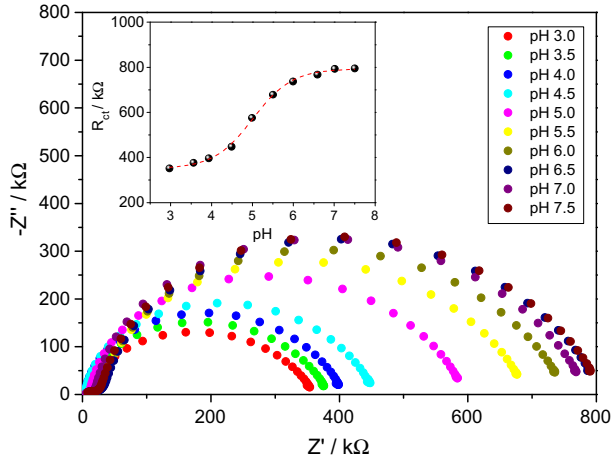

Fig. 4. Nyquist plots of a 4NTP/4MBA SAM modified gold electrode in the presence of 1.0 mmol L^{-1} $[Fe(CN)_6]^{3-}$ at pH 3.5, 4.0, 4.5, 5.0, 5.5, 6.0, 6.5, 7.0, 7.5, and 8.0 solutions of 0.1 mol L^{-1} ionic strength. Insert: (•) faradaic impedance titration plots for 4NTP/4MBA SAM modified gold electrode and calculated plot based on Eq. (14).

increases. The R_{ct} vs pH plot exhibits a sigmoidal shape indicating the applicability of R_{ct} to take information about the fractional degree of acidic or basic groups on the surface and the plot can be viewed as a direct titration curve, as recently verified by Kim and Kwak [47] for single and mixed SAM. The titration curve for acidic groups presents two main features when compared with the same titration curve for acid molecules in solution. First, the solution pH at which the R_{ct} is midway between the plateau at high and low pH (surface pK_{ap}) is 5.0, which is about 2 units higher than the pK_{ap} measured for similar acids in bulk aqueous solution [48]. Second, the titration curve is broader (extending from 4.5 up to 5.5) than those observed for monocarboxylic acids in aqueous solutions, which is in agreement to the previous results for similar systems investigated by different methods [47,49].

The apparent pK_{ap} increases and the broadening of the titration curve can be associated with many particular aspects of surface grafted thiol molecules, including strong intermolecular lateral hydrogen bonding between the surface molecules [50]. Hydrogen bond formation causes the acidic protons to be held more tightly on the monolayer surface and deprotonation of an acid layer is energetically unfavorable because of the high electrostatic repulsion that the neighboring ionized carboxylate groups experience at the monolayer/solution interface. On the other hand, the broadening of the titration curve can be explained by a theoretical model, which takes into account the effect of electrostatic interaction, predicting the broadening of the titration curve. To explain the effects of the interaction between the terminal groups of the molecules and ions in the solution, Smith and White [51] revisited these systems and proposed a theoretical model that related the total capacitance of metal electrodes coated with acid or base monolayer films to the applied potential and solution pH.

Briefly, the basis of this model is the assumption that all acid/base groups lie in the common plane, referred to as the "plane of acid dissociation" (PAD), and defined Ψ as the potential drop between the PAD and the bulk solution as represented in following equation:

$$\log\left(\frac{\theta}{1-\theta}\right) = \mathrm{pH} - \left(\frac{\mathrm{p}K_{ap} - F\psi}{2.3RT}\right) \quad (13)$$

where θ is the fraction of ionized molecules in the monolayers and K_a is the dissociation constant of the surface-bound acid groups when $\Psi = 0$. From Eq. (13) and the definition of apparent pK_{ap} (pH value when half of the surface-grafted acid groups is ionized), it follows that $pK_{ap} = pH - F\Psi/2.3RT$.

To investigate the in-plane electrostatic force effect on the surface pK_{ap}, the dependence of the titration curve has been considered. For this, the titration curve (i.e. R_{ct} vs pH) is compared with the plot of the theoretical prediction (i.e. θ vs pH). With the increase of θ, the surface potential Ψ is shifted to more negative values, because of the increase of the repulsive force between charged acids in a SAM. The Ψ change as a function of θ results in the broadening of the titration curve. Neglecting the dependence of Ψ upon θ, by replacing $(pK_{ap} - F\Psi/2.3RT)$ of Eq. (13) by 5.0, which is the experimentally determined $pK_{1/2}$ for the pure MPA monolayer, we can rewrite Eq. (13):

$$\log\left(\frac{\theta}{1-\theta}\right) = pH - 5.0 \quad (14)$$

The titration curve observed experimentally would be broader than the plot by Eq. (14) if the effect on the surface pK_{ap} were significant. The Inset of Fig. 4 (dashed line) shows the best fit between the experimental and theoretical (based on Eq. (14)). Considering that the observed shift of the pK_a is mainly due to electrostatics and hydrogen bonding, the 'dilution' of the carboxylic acid groups with pTNP thiols should decrease the surface pK_{ap} for acid groups. Therefore, these investigations about the surface pK_{ap} show the relevance of the full control of the surface properties, which can influence the capability of the 4NTP SAM toward the analyte. Then, pure and mixed SAMs were tested toward the ascorbic acid, epinephrine and uric acid electrochemical selectivity.

These investigations about the pK_a's surface show the relevance of the control of surface properties. Being the pK_a of AA is 4.17, uric acid's is 5.75 and epinephrine's is 8.89, it becomes clear why the selectivity of mixed SAM proposed. About the titration curve of surface groups is clear that at pH 5.5, SAM displays the carboxylic groups in the anionic form. On the other hand, at this same pH, AA is negatively charged while epinephrine and uric acid are protonated. Therefore, the electrostatic repulsion between SAM and AA may be the main factor that favors the selective behavior of the system. Therefore, for further experiments pH 5.5 was chosen to avoid AA interference on the EP and UA response.

3.4. Electrochemical determination of EP and UA in the presence of AA

The ability of the modified electrode to promote the voltammetric resolution of EP, and UA in the presence of AA was investigated. The electrochemical determination of EP using bare electrodes suffers from interference by UA and AA because the oxidation potential of UA and AA are fairly close to EP [31]. Fig. 5a shows the differential pulse voltamograms obtained at the bare electrode, 4NTP SAM, 4MBA, and 4NTP/4MBA SAM in 0.1 mol L^{-1} phosphate buffer solution (pH 5.5) containing 90 μmol L^{-1} UA, 0,825 μmol L^{-1} EP, and 1 mmol L^{-1} AA. The modification of electrode surface with 4NTP/4MBA SAM resolved the merged voltammetric peak observed on bare gold electrode into two well-defined voltammetric peaks at potentials around 0.120 and 0.475 V vs Ag/AgCl for EP and UA, respectively.

In order to establish a sensitive and selective method for the quantification of EP and UA in the presence of AA, two different experiments were carried out at 0.1 mol L^{-1} phosphate buffer solution (pH 5.5). In each experiment, the concentration of one of the two compounds was changed while the concentrations of the other were kept constant. These experiments were carried out in the presence of 1 mmol L^{-1} of AA.

As shown in Fig. 5b, the peak current of EP increased linearly with increasing EP concentration in the range of 100–825 nmol L^{-1} in the presence of 1 mmol L^{-1} AA and 90 μmol L^{-1} UA. No significant

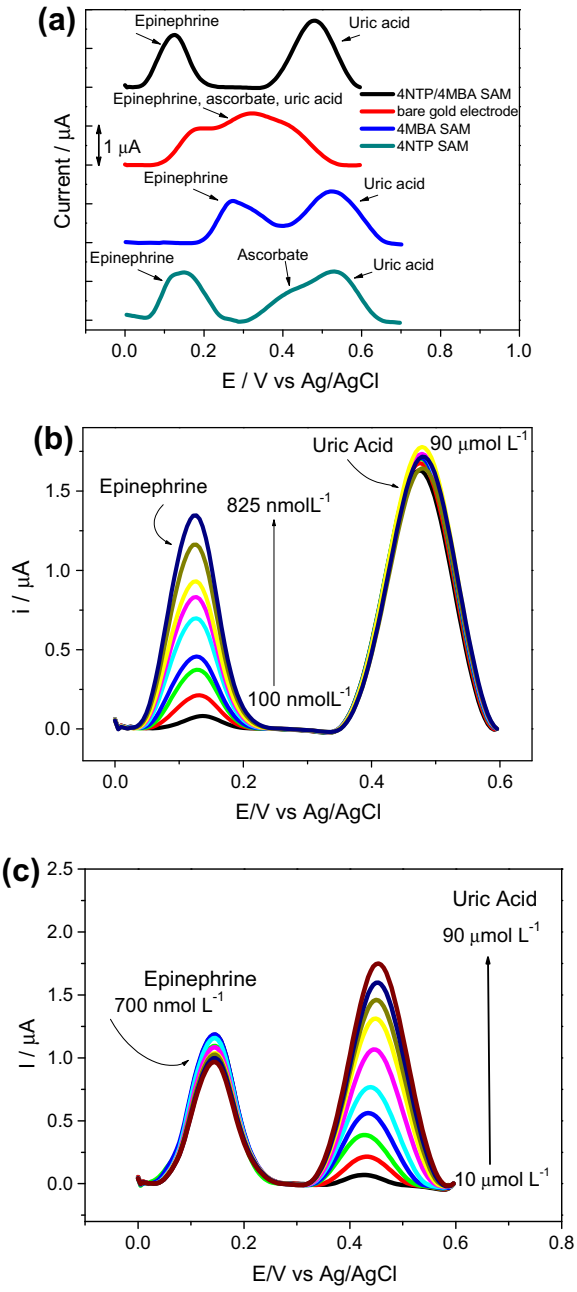

Fig. 5. (a) Differential pulse voltamograms obtained at the bare electrode, 4NTP SAM, 4MBA, and 4NTP/4MBA SAM in 0.1 mol L^{-1} phosphate buffer solution (pH 5.5) containing 90 µmol L^{-1} UA and 0, 825 µmol L^{-1} EP, and 1 mmol L^{-1} AA; (b) differential pulse voltammograms of the 4NTP/MBA SAM modified electrode in 0.1 mol L^{-1} phosphate buffer solution (pH 5.5) containing 90 µmol L^{-1} UA and different concentrations of EP: 100, 200, 290, 385, 475, 565, 655, 740, 825 nmol L^{-1}; (c) containing 700 nmol L^{-1} EP, and different concentrations of UA: 10.0, 19.5, 29.0, 38.5, 47.6, 56.6, 65.4, 74.1, 82.6, 90.9 µmol L^{-1}. 1 mmol L^{-1} AA.

change was observed in the UA oxidation currents. The peak current of UA was investigated in the presence of 700 nmol L^{-1} EP and 1 mmol L^{-1} AA. Fig. 5c depicts the response from additions of UA in the range of 10–90 µmol L^{-1}. No significant interference was observed in the EP oxidation current. No change was observed upon addition of the AA in the range of 100–1000 µmol L^{-1}. These results showed that the 4NTP/4MBA SAM modified electrode has good sensitivity and selectivity, and independent or simultaneous determination of EP and UA is possible without any interference from each other as well as from AA.

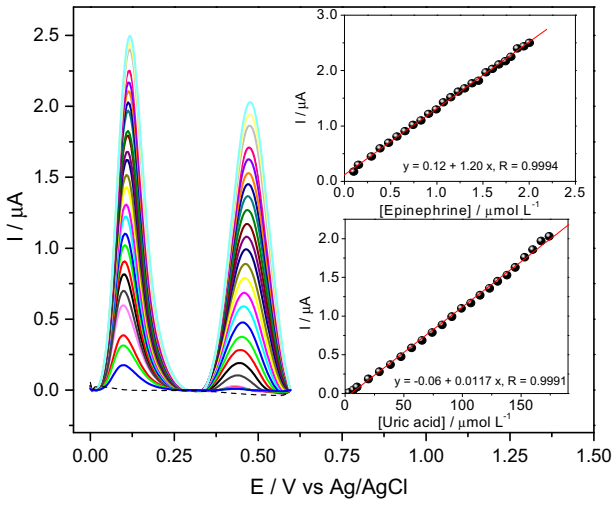

Fig. 6. Differential pulse voltammograms of the 4NTP/4MBA SAM modified electrode in 0.1 mol L^{-1} phosphate buffer solution (pH 5.5) at different concentrations of EP (0.1, 0.15, 0.29, 0.38, 0.48, 0.57, 0.65, 0.74, 0.83, 0.91, 0.99, 1.07, 1.15, 1.23, 1.30, 1.38, 1.45, 1.53, 1.60, 1.67, 1.74, 1.80, 1.87, 1.94, 2.00 µmol L^{-1}) and UA (1, 3, 7, 10, 20, 29, 38, 48, 57, 65, 74, 83, 91, 99, 107, 115, 123, 130, 138, 145, 153, 160, 167, 174 µmol L^{-1}). Insets: the calibration curves for EP and UA. Scan rate: 50 mV s^{-1}; pulse amplitude: 50 mV. 1 mmol L^{-1} AA (dashed line).

The effects of the scan rate and the pulse amplitude on the DPV response of 4NTP/4MBA SAM modified electrode were also investigated in 0.1 mol L^{-1} phosphate buffer solution (pH 5.5) (data not shown). The better voltammetric sensitivity toward EP was obtained for a scan rate of 0.05 V s^{-1} and pulse amplitude of 0.05 V.

Under optimized conditions, the DPV of the ternary mixture of EP and UA in presence of 1 mmol L^{-1} of AA were recorded (Fig. 6) and the analytical curves were obtained (Inset Fig. 6). The relationship between peak current and concentration of EP was linear in the range of 0.1–2 µmol L^{-1} with a linear equation of I_{pa} (µA) = 0.12 + 1.12 [EP] (µmol L^{-1}) (r = 0.999), and a detection limit of 37 nmol L^{-1}. For UA, the calibration curve was linear in the range of 1–175 µmol L^{-1} with a linear equation of I_{pa} (µA) = −0.06 + 0.0117 [UA] (µmol L^{-1}) (r = 0.999), and a detection limit of 0.5 µmol L^{-1}. As shown, the 4NTP/4MBA SAM modified electrode is highly sensitive, especially in relation to EP and UA when compared with previous results reported in literature (Table 1).

The stability of 4NTP/4MBA SAM modified electrode was checked in the presence of 1 µmol L^{-1} EP and 100 µmol L^{-1} UA performing successive voltammetric measurements in 0.1 mol L^{-1} phosphate buffer solution (pH 5.5). After 100 voltammetric measurements no change was observed in the voltammetric profiles of the modified electrode. When the modified electrode was stored at room temperature, no significant change in the response was observed for at least 1 month.

The modified electrode presented a good repeatability for EP and UA determination. The relative standard deviation (R.D.S.) for ten determinations of 100 nmol L^{-1} EP and 250 µmol L^{-1} UA in a binary mixture was 0.5% and 2.5% for EP and UA, respectively. Additionally, a series of ten modified electrodes prepared in the same manner was also tested at phosphate buffer (pH 5.5) containing 100 nmol L^{-1} EP and 250 µmol L^{-1} UA. The relative standard deviation observed was less than 5.0% for each one. These results indicate that the 4NTP/4MBA SAM modified electrode have good stability and repeatability, probably due to the ability of gold electrode in fixing 4NTP and MBA molecules on the electrode surface in a stable and reproducible way.

Table 1
Comparison of some characteristics of the different modified electrodes for the simultaneous determination of EP and UA.

Modified electrode	E_{oxi} (V)			LOD (μmol L^{-1})		Linear range (μmol L^{-1})		Sensitivity (μA/μmol L^{-1})		Ref.
	EP	UA	ΔEp (EP-UA)	EP	UA	EP	UA	EP	UA	
Activated glassy carbon electrode	0.190	0.350	0.160	0.089	0.16	1.00–40.00	1.00–55.00	0.17	0.0949	[52]
DPDSAM	0.170	0.390	0.220	0.51	9.0	0.7–500	10–750	0.009	0.010	[53]
Sonogel-carbon electrode	0.237	0.438	0.201	0.087	–	0.1–500	–	0.0521	–	[54]
MDWCNTPE	0.065	0.280	0.215	0.216	8.8	0.7–1200	25–750	0.3693 and 0.0148	0.0147	[55]
BMPTB/CPE	0.160	0.320	0.160	0.050	–	–	50–175	–	–	[56]
Mixed 4NTP/4MBA	0.120	0.475	0.355	0.037	0.5	0.1–2.0	1.0–175	1.20	0.0117	This work

DPDSAM – gold electrode modified by 2-(2,3-dihydroxy phenyl)-1,3-dithiane self-assembled monolayer; TMBH SAM – [2-hydroxy-N′1-[(E)-1-(3-methyl-2-thienyl) methylidene] benzohydrazide self-assembled monolayer modified gold electrode; 2,2′-[1,2-ethanediylbis(nitriloethylidyne)]-bis-hydroquinone double-wall carbon nanotube paste electrode; BMPTB/CPE – 1-butyl-4-methyl-pyridinium tetrafluroborate ionic liquid modified carbon paste electrode.

4. Conclusions

In this work, a novel sensor was developed by a strongly adsorption of 4NTP/4MBA SAM on gold electrode. The modified electrode exhibited highly sensitivity for the oxidation of EP and UA in presence of AA. Two-well defined peaks were observed in DPV at low potentials as 0.150 and 0.450 V vs Ag/AgCl, respectively. Electron transfer of 4NTP/4MBA SAM before and after activation was studied by SECM and it is evident that electrochemically triggered surface confined reaction is of high importance on the sensitivity of the mixed SAM response. We have studied the effects of the surface pK_a on the selectivity 4NTP/4MBA mixed SAMs using faradaic impedance titration. The detection limit and sensibility for EP as well as the selectivity to EP and UA were much better than those described in the literature. Moreover, this sensor showed good repeatability and stability for the measurements. Therefore, the proposed method can be applied to the individual or simultaneous determination of these compounds with satisfactory results.

Acknowledgments

The authors are grateful to Conselho Nacional de Desenvolvimento Científico e Tecnológico (CNPq), Rede Mineira de Química, INCT-Bio and Fundação de Amparo à Pesquisa do Estado de Minas Gerais (FAPEMIG) for financial support.

References

[1] J.C. Ndamanisha, L.-p. Guo, Anal. Chim. Acta 747 (2012) 19–28.
[2] A. Afzal, N. Cioffi, L. Sabbatini, L. Torsi, Sensor. Actuat. B 171–172 (2012) 25–42.
[3] A. Liu, K. Wang, S. Weng, Y. Lei, L. Lin, W. Chen, Xi. Lin, Y. Chen, TrAC Trends Anal. Chem. 37 (2012) 101–111.
[4] A.L. Eckermann, D.J. Feld, J.A. Shaw, T.J. Meade, Coord. Chem. Rev. 254 (2010) 1769–1802.
[5] L. Srisombat, A.C. Jamison, T.R. Lee, Colloids Surface A 390 (2011) 1–19.
[6] S.K. Arya, P.R. Solanki, M. Datta, B.D. Malhotra, Biosens. Bioelectron. 24 (2009) 2810–2817.
[7] A. Turchanin, A. Gölzhäuser, Prog. Surf. Sci. 87 (2012) 108–162.
[8] E. Scavetta, A.G. Solito, M. Demelas, P. Cosseddu, A. Bonfiglio, Electrochim. Acta 65 (2012) 159–164.
[9] W. Chen, S. Hong, H.B. Li, H.Q. Luo, M. Li, N.B. Li, Corros. Sci. 61 (2012) 53–62.
[10] A.V. Rudnev, K. Yoshida, T. Wandlowski, Electrochim. Acta 87 (2013) 770–778.
[11] S.M. Rosendahl, I.J. Burgess, Electrochim. Acta 56 (2011) 4361–4368.
[12] J.C. Love, L.A. Estroff, J.K. Kriebel, R.G. Nuzzo, G.M. Whitesides, Chem. Rev. 105 (2005) 1103–1169.
[13] J.-J. Shyue, M.R. De Guire, T. Nakanishi, Y. Masuda, K. Koumoto, C.N. Sukenik, Langmuir 20 (2004) 8693–8698.
[14] V. Dupres, C. Verbelen, Y.F. Dufrêne, Biomaterials 28 (2007) 2393–2402.
[15] T.T.-C. Tseng, H.G. Monbouquette, J. Electroanal. Chem. 682 (2012) 141–146.
[16] X. Zhang, L. Liu, X.Y. Zhang, K. Ma, Y. Rao, Q. Zhao, F. Li, J. Pharm. Biomed. Anal. 59 (2012) 1–12.
[17] D.T. Marc, J.W. Ailts, D.C.A. Campeau, M.J. Bull, K.L. Olson, Neurosci. Biobehav. Rev. 35 (2011) 635–644.
[18] C.E. Teunissen, J. de Vente, H.W.M. Steinbusch, C.D. Bruijn, Neurobiol. Aging 23 (2002) 485–508.
[19] J.J. Rodríguez, H.N. Noristani, A. Verkhratsky, Prog. Neurobiol. (N.Y.) 99 (2012) 15–41.
[20] G. Zhang, Y. Zhang, C. Ji, T. McDonald, J. Walton, E.A. Groeber, R.C. Steenwyk, Z. Lin, J. Chromatogr. B: Anal. Technol. Biomed. Life Sci. 895–896 (2012) 186–190.
[21] E.V. Efremov, F. Ariese, C. Gooijer, Anal. Chim. Acta 606 (2008) 119–134.
[22] T. Li, Z. Wang, H. Xie, Z. Fu, J. Chromatogr. B: Anal. Technol. Biomed. Life Sci. 911 (2012) 1–5.
[23] Y. Zhao, S. Zhao, J. Huang, F. Ye, Talanta 85 (2011) 2650–2654.
[24] A.V. Bulatov, A.V. Petrova, A.B. Vishnikin, A.L. Moskvin, L.N. Moskvin, Talanta 96 (2012) 62–67.
[25] F. Cui, X. Zhang, J. Electroanal. Chem. 669 (2012) 35–41.
[26] X. Liu, D. Ye, L. Luo, Y. Ding, Y. Wang, Y. Chu, J. Electroanal. Chem. 665 (2012) 1–5.
[27] R.N. Goyal, A.R.S. Rana, H. Chasta, Electrochim. Acta 59 (2012) 492–498.
[28] T. Luczak, Electrochim. Acta 54 (2009) 5863–5870.
[29] H. Harper, A Review of Physiological Chemistry, Lange Medical, Los Altos, California, 1977.
[30] S. Behera, C.R. Raj, Sensors Actuat. B 128 (2007) 31–38.
[31] A. Sivanesan, S.A. John, Electroanalysis 20 (2008) 2340–2346.
[32] S. Shahrokhian, M. Ghalkhani, M.K. Amini, Sensors Actuat. B 137 (2009) 669–675.
[33] Bernard A. Boukamp, Solid State Ionics 169 (2004) 65–73.
[34] W. Kemula, T.M. Krygowski, in: A.J. Bard, H. Lund (Eds.), Encyclopedia of Electrochemistry of the Elements. Organic Section, vol. 23, Dekker, New York, 1979, p. 77 (Chapter 2).
[35] M.R. Lindbeck, H. Freund, Anal. Chim. Acta 35 (1966) 74–84.
[36] E. Casero, M. Darder, K. Takada, H.D. Abruña, F. Pariente, E. Lorenzo, Langmuir 15 (1999) 127–134.
[37] A.J. Bard, L.R. Falkner, Electrochemical Methods Fundaments and Applications, second ed., Wiley, 2001.
[38] J.F. Smalley, H.O. Finklea, C.E.D. Chidsey, M.R. Linford, S.E. Creager, J.P. Ferraris, K. Chalfant, T. Zawodzinsk, S.W. Feldberg, M.D. Newton, J. Am. Chem. Soc. 125 (2003) 2004–2013.
[39] H.D. Sikes, J.F. Smalley, S.P. Dudek, A.R. Cook, M.D. Newton, C.E.D. Chidsey, S.W. Feldberg, Science 291 (2001) 1519–1523.
[40] E. Laviron, J. Electroanal. Chem. 101 (1979) 19–28.
[41] C. Wei, A.J. Bard, M.V. Mirkin, J. Phys Chem. 99 (1995) 16033–16042.
[42] M.V. Mirkin, F.R.F. Fan, A.J. Bard, J. Electroanal. Chem. 328 (1992) 47–62.
[43] B. Liu, A.J. Bard, M.V. Mirkin, S.E. Creager, J. Am. Chem. Soc. 126 (2004) 1485–1492.
[44] A. Kiani, M.A. Alpuche-Aviles, P.K. Eggers, M. Jones, J.J. Gooding, M.N. Paddon-Row, A.J. Bard, Langmuir 24 (2008) 2841–2849.
[45] K.B. Holt, Langmuir 22 (2006) 4298–4304.
[46] S.E. Salamifar, M.A. Mehrgardi, S.H. Kazemi, M.F. Mousavi, Electrochim. Acta 56 (2010) 896–904.
[47] K. Kim, J. Kwak, J. Electroanal. Chem. 512 (2001) 83–91.
[48] T. Kakiuchi, M. Iida, S.-i. Imabayashi, K. Niki, Langmuir 16 (2000) 5397–5401.
[49] P.S. Hale, L.M. Maddox, J.G. Shapter, J.J. Gooding, J. Chem. Educ. 82 (2005) 779–785.
[50] K. Aoki, T. Kakiuchi, J. Electroanal. Chem. 478 (1999) 101–107.
[51] C.P. Smith, H.S. White, Langmuir 9 (1993) 1–3.
[52] J.X. Qiao, H.Q. Luo, N.B. Li, Colloids Surfaces B: Biointerface 62 (2008) 31–35.
[53] M. Mazloum-Ardakani, H. Beitollahi, M.K. Amini, B.-F. Mirjalili, F. Mirkhalaf, J. Electroanal. Chem. 651 (2011) 243–249.
[54] H.E. Bouhouti, I. Naranjo-Rodríguez, J.L.H.-H. de Cisneros, M. ElKaoutit, K.R. Temsamani, D. Bouchta, L.M.C. Aguilera, Talanta 79 (2009) 22–26.
[55] Hadi Beitollahi, Mohammad Mazloum Ardakani, Bahram Ganjipour, Hossein Naeimi, Biosens. Bioelectron. 24 (2008) 362–368.
[56] B.N. Chandrashekar, B.E.K. Swamy, N.B. Ashoka, M. Pandurangachar, J. Mol. Liq. 165 (2012) 168–172.